MALDI versus DESI mass spectrometry imaging of lipids in atherosclerotic plaque

Slijkhuis, Nuria; Towers, Mark; Claude, Emmanuelle; van Soest, Gijs

DOI
10.1002/rcm.9927

Publication date
2025

Document Version
Final published version

Published in
Rapid Communications in Mass Spectrometry

Received: 10 July 2024 | Revised: 2 October 2024 | Accepted: 2 October 2024

DOI: 10.1002/rcm.9927

RESEARCH ARTICLE

Rapid Communications in Mass Spectrometry WILEY

MALDI versus DESI mass spectrometry imaging of lipids in atherosclerotic plaque

Nuria Slijkhuis[1] | Mark Towers[2] | Emmanuelle Claude[2] | Gijs van Soest[1,3,4]

[1]Department of Cardiology, Cardiovascular Institute, Thorax Center, Erasmus MC, Rotterdam, The Netherlands

[2]Waters Corporation, Wilmslow, UK

[3]Department of Precision and Microsystems Engineering, Delft University of Technology, Delft, The Netherlands

[4]Wellman Center for Photomedicine, Massachusetts General Hospital, Boston, Massachusetts, USA

Correspondence
Gijs van Soest, Department of Cardiology, Cardiovascular Institute, Thorax Center, Erasmus MC, Rotterdam, The Netherlands.
Email: g.vansoest@erasmusmc.nl

Funding information
NWO, Grant/Award Number: Vici 16131

Mass spectrometry imaging (MSI) is a powerful tool for detecting lipids in tissue sections, with matrix-assisted laser desorption/ionization (MALDI) and desorption electrospray ionization (DESI) as its key ionization techniques. In this study, we examine how MALDI compares with state-of-the-art DESI ionization in identifying lipids in heterogeneous samples, specifically atherosclerotic plaques. Carotid plaques ($n = 4$) from patients undergoing endarterectomy were snap-frozen, stored at −80°C, and then sectioned for MSI analysis and H&E staining. Measurements were conducted using a SYNAPT XS mass spectrometer in positive ion mode, employing MALDI with a 2,5-dihydroxybenzoic acid (DHB) matrix and DESI with a methanol: water (*98:2*) (*v/v*) solvent. Our comparison covered spectral profiles, sensitivity, and image quality generated by these two techniques. We found that both MALDI and DESI are highly suitable techniques for detecting a wide range of lipids in atherosclerotic plaque sections. DESI-MSI exhibited higher ion counts for most lipid classes than MALDI-MSI and provided sharper images. MALDI detected larger amounts of ceramide and hexosylceramide species, possibly due to its efficient generation of dehydrated ions. In contrast, DESI showed greater peak intensities of cholesteryl ester and triacylglyceride species than MALDI, consistent with reduced fragmentation. These findings establish the relative merits of DESI and MALDI and demonstrate their complementarity as techniques for lipid research in MSI.

1 | INTRODUCTION

Lipidomics is a technique widely used for lipid analysis in a variety of biomedical research scenarios and increasingly in clinical settings.[1,2] While this methodology is suitable for liquid samples or homogeneous tissue extracts, it does not capture the heterogeneous lipid distribution in tissues. A highly suitable technique for the detection of lipids while preserving their distribution is mass spectrometry imaging (MSI). MSI is a molecular imaging technique that can detect a wide range of lipids in situ in a label-free manner. The surface of the sample is probed with a stream of particles, which can be photons, primary ions, or charged microdroplets depending on the ionization technique used.[3] During acquisition, molecules are desorbed from the sample surface, ionized, and measured based on their mass-to-charge ratio (*m/z*). A mass spectrum per sampling position (pixel) is generated, preserving the location of each ion across the sampled area, which makes it possible to reconstruct images of the spatial distribution of each detected molecule.

The most commonly used ionization technique in MSI is matrix-assisted laser desorption/ionization (MALDI).[4–6] MALDI-MSI has been used extensively for the detection of lipids in different tissue types.[6] MALDI involves the deposition of a thin organic matrix layer on the sample, which crystallizes analytes in tissue sections and aids in their ionization when exposed to laser irradiation. The selection of the matrix and the details of its application can be optimized toward the detection of compounds of interest, albeit at the cost of

sensitivity to other species. MALDI has been realized both under high vacuum and atmospheric pressure. High vacuum conditions yield a greater number of *m/z* features but could cause the loss of volatile compounds from the sample.[7] Matrix-related ions can increase spectral complexity, as these additional compounds contribute unrelated signals that can complicate data interpretation.[8]

Desorption electrospray ionization (DESI) was one of the first ambient ionization techniques introduced in 2004,[9] relying on a fine spray of charged microdroplets for desorption and ionization of the molecules. Despite its growing popularity since then,[10–12] DESI has not reached the same level of widespread use as MALDI-MSI. Nonetheless, there are several features that merit consideration as a routine MSI technique in addition to MALDI: DESI requires no sample preparation and is a "softer" ionization technique, due to the low-impact ionization probe, which limits in-source fragmentation of molecules.[13] However, its sensitivity and spatial resolution have lagged those of MALDI, and optimization of the spray required significant user experience. Recent technological improvements in DESI-MSI are bridging this gap, significantly enhancing both its sensitivity and spatial resolution.[14,15]

Atherosclerosis is a lipid- and inflammation-driven disease of the arteries.[16] Lipids accumulate in the vessel wall leading to the formation of so-called plaques. When these plaques rupture, a thrombus is formed, which can partly, or completely, block the blood flow leading to a transient ischemic attack, ischemic stroke, or myocardial infarction depending on the location of the plaque. The risk of a plaque rupturing depends on its biomechanical tissue composition, which may be highly influenced by the type of lipid present. Because lipids play a pivotal role in plaque progression, characterizing these lipids in plaques can aid in the understanding of the disease.

Both MALDI[17–21] and DESI[22–24] have been applied to studying lipid distributions in atherosclerotic plaques. In this study, we compare the suitability of the "gold standard" MALDI versus DESI ionization in detecting lipids within heterogeneous samples, such as atherosclerotic plaques. Employing the same mass spectrometer, equipped with a MALDI and DESI source, we analyzed an identical set of atherosclerotic plaque sections ($n = 4$). Our comparison covers spectral profiles, sensitivity, and image quality generated by these two techniques.

2 | METHODS

2.1 | Sample collection and preparation

Carotid plaques ($n = 4$) were collected from patients undergoing carotid endarterectomy. Plaques were immediately snap-frozen upon collection and stored at −80°C until further processing. Subsequently, plaques were cut into 3 mm cross-sections, which were embedded in 10% porcine type A gelatin. The cross-sectional block with the highest plaque burden was selected for MSI measurements and cryosectioned in 10 µm thick sections. Two sections were used for DESI- and MALDI-MSI, and consecutive sections were used for histology.

2.2 | DESI AND MALDI-MSI

MALDI-MSI measurements were performed on a SYNAPT XS mass spectrometer with a MALDI source in positive ionization mode. An organic matrix of 2,5-dihydroxybenzoic acid (DHB) was spray-coated using a Sunchrom SunCollect sprayer. Briefly, DHB >99.0% (Sigma Aldrich) 10 mg/mL in 70% Acetonitrile (aq) was sprayed at 20 µL per min. Twenty-five layers were applied with a line spacing of 1.5 mm, and a nebulizing gas (nitrogen) was used at 1.7 bar. For MALDI analysis the small spot mode was used (approximately 45 µm on sample burn width), and the laser attenuation was adjusted to maximize signal while limiting in-source fragmentation. The laser was operated at 1 kHz with 500 shots per position, and the total acquisition time per pixel was 0.5 s.

DESI-MSI measurements were performed on a SYNAPT XS mass spectrometer with a DESI XS source (Waters, Wilmslow, UK) in positive ionization mode. DESI spray solvent was methanol: water 98:2 (%*v*/*v*) (Honeywell, Germany), which was delivered with a solvent flow rate of 2 µL/min. The capillary voltage was optimized between 0.6 and 0.8 kV, and the nitrogen gas pressure was 69–103 kPa (10–15 psi). A heated transfer line was used at 370°C to improve ionization and transmission of the molecules into the mass spectrometer. The DESI data were acquired at two pixels per second giving a total scan time of 0.486 s per pixel (0.5 s cycle time—interscan delay).

Both MALDI and DESI measurements were performed in sensitivity mode with a pixel size of 100 × 100 µm^2. For MALDI, the data were acquired using discrete positional sampling, whereas for DESI, a continuous method of movement was used.

In both cases, the data were acquired with a degree of under-sampling. For the MALDI analysis, the Synapt XS MALDI source was fine-tuned to achieve a burn diameter of approximately 45 µm by using the small spot position and precisely adjusting the laser attenuation. This burn diameter of 45 µm has been previously established for this source based on a circular desorption area.[25] This corresponds to a sampling area of 1,590 µm^2 per pixel, which covers 15.9% of the defined 100 × 100 µm pixel area. For DESI, precisely determining the desorption area is challenging. Using a high-performance sprayer,[14] the solvent plume diameter has been estimated to range between 20 and 25 µm, based on previous studies with optimized gas settings and a solvent flow rate of 2 µL/min.[26,27] Assuming this results in a circular desorption area of 20–25 µm on the tissue, the sampling area would be approximately 314.16 to 490.87 µm^2. Unlike MALDI, where each pixel corresponds to a set of laser shots on a discrete position, DESI acquires data using a continuous raster across the pixel. This results in a total sampled area per pixel of approximately 2314.16 to 2990.87 µm^2, or 23.14% to 29.9% of the defined pixel area. A visualization of these area calculations is provided in Figure S1.

For DESI, the overall signal is expected to be higher than for MALDI due to the continuous extraction and desorption process. In contrast, MALDI relies on analyte extraction at the point of matrix application, which limits the extraction efficiency based on the matrix application method. In this case, due to the low resolution of

the imaging experiments, for MALDI, a wet matrix application method was employed increasing matrix drying time and maximizing analyte extraction.

The mass range was *m/z* 100–1200, and the scan acquisition rate was two scans per second. Data were acquired using MassLynx v4.2 software. Continuous lock mass correction was performed on the raw data using a prominent and known lipid species, namely, SM(34:1) $[M + Na]^+$ (*m/z* 725.5). HDI v1.7 software was used to export the data in imzML format (Waters, Wilmslow, UK). An in-house data processing pipeline[28] in MATLAB™ 2017a (The Mathworks, Inc., Natick, Massachusetts, USA) was used in combination with mMass software[29] to select lipid *m/z* features and remove isotopes. In mMass, an S/N threshold of 10.0 and a peak-picking height of 80% was applied. This was performed on the base peak spectrum because of the heterogeneous nature of the atherosclerotic plaques. For further data analysis, a subset of lipid *m/z* features was selected that were present in at least two out of four samples.

2.3 | Histology

Adjacent tissue sections to those analyzed by DESI and MALDI-MSI were stained by hematoxylin & eosin (HE) (VWR, The Netherlands). Whole slides were digitized with a Nanozoomer 2.0 HT slide scanner (Hamamatsu Photonics, Hamamatsu, Japan) at 20X magnification with a pixel size of 0.455 µm.

2.4 | Lipid annotation

A list of lipid species in plaque homogenates was generated using the Lipidyzer platform, which separates lipid classes via differential mobility spectrometry, followed by multiple reaction monitoring. Quantification is performed using 54 deuterated internal standards and an automated informatics approach.[30] The data includes m/z values for [M-H + H2O] +, [M + H]+, [M + Na]+, and [M + K] + adducts. In the MALDI and DESI data, lipid-related *m/z* features were annotated based on matches with this list. In addition, known m/z features for lipids that are not in the Lipidyzer standard set but were annotated in previous experiments by matching to high-mass-resolution MALDI-FTICR-MSI[17] (e.g., cholesterol and its derivatives; long-chain phosphatidylcholines, oxidized cholesteryl esters, saturated sphingomyelins, and ceramides) were tentatively assigned based on exact mass, matched to the Lipid Maps database. Annotations with parts per million (ppm) mass error below 15 were retained.

3 | RESULTS

3.1 | Number of detected lipids with MALDI/DESI

We detected 351 lipid-related m/z features with MALDI-MSI and 357 lipid-related *m/z* features with DESI-MSI. Of these m/z features, 185 and 194 *m/z* in total could be annotated for MALDI and DESI, respectively; see Table S1. For the two techniques, 114 (62%) and 131 (68%) features were annotated based on the plaque lipidomics data set (highlighted in Table S1). Annotations include all ionization states (e.g., $[M + H]^+$, $[M + Na]^+$, $[M + K]^+$), which means some identical annotations can occur in different forms. When considering the unique annotations exclusively, there are 138 and 150 unique annotations for MALDI and DESI, respectively. Among these unique lipid annotations, 85 lipids were detected by both MALDI and DESI, whereas 53 annotations were exclusive to MALDI, and 65 were uniquely detected by DESI; see Figure 1.

Lipids belonged to eight different lipid classes, namely, sterols (ST), ceramides (Cer), hexosylceramides (HexCer), lactosylceramides (Hex2Cer), sphingomyelins (SM), phosphatidylcholines (PC), lysophosphatidylcholines (LPC), cholesteryl esters (CE), diacylglycerides (DG), and triacylglycerides (TG). When considering the total number of lipid annotations, MALDI-MSI detected relatively more SM, Cer, and HexCer species—25, 12, and 10, respectively—compared to DESI-MSI, which detected 18 SM, 8 Cer, and 2 HexCer species. While with DESI, we detected relatively more CE, DG, and TG species, namely, 19, 27, and 63, compared to 13 CE, 22 DG, and 25 TG species with MALDI. However, when distinguishing between total and unique lipid species—the latter counting each lipid molecule only once regardless of its ionization state (e.g., [M + H] + vs. [M + Na]+)—the perspective changes for some lipid classes. Specifically, the difference in unique SM species between the techniques narrows significantly to 14 for MALDI versus 12 for DESI, largely because several SM species were detected in both the protonated form and the sodiated form with MALDI. Similarly, while the initial count suggested a higher detection of DG species by DESI, the number of unique DG species is equal between DESI and MALDI since the observed differences in the total counts were influenced by DESI detecting many DG species as distinct ions. The unique number of PC species is slightly higher for MALDI compared to DESI, namely, 33 versus 28, respectively. For sterols and

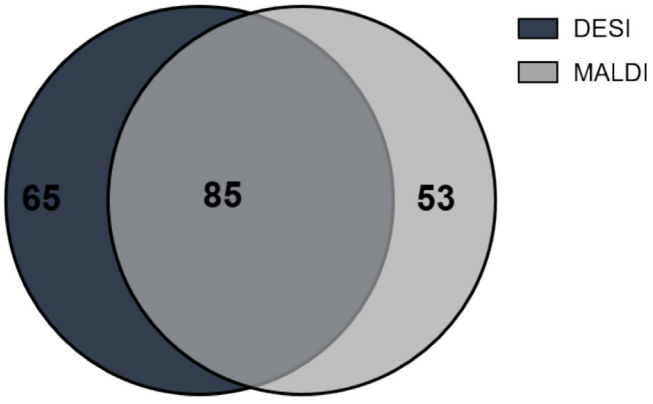

FIGURE 1 Number of overlapping and unique lipid species in desorption electrospray ionization (DESI) and matrix-assisted laser desorption/ionization (MALDI). m/z with the same lipid annotation but different ion forms were only counted once. [Color figure can be viewed at wileyonlinelibrary.com]

LPC classes, no notable differences were observed in the counts of unique species between MALDI and DESI. Specifically, both methods identified four unique sterol species each, while the numbers for LPCs were similar, namely, 13 for MALDI versus 14 for DESI. Figure 2 provides an overview of both the total and unique numbers of species per lipid class identified by MALDI and DESI.

3.2 | Sensitivity and image quality

The comparative analysis of DESI and MALDI MSI techniques revealed notable differences in sensitivity and image quality, as illustrated by the data presented in Figures 3 through 5. Figure 3 depicts the mass spectra for a representative plaque sample, with several lipid species indicated. Notably, the absolute intensity of the peaks detected by DESI was markedly higher, with intensities reaching up to 350 000, compared to a maximum of 80 000 observed in MALDI spectra.

Further quantitative assessment of the intensity differences across all four samples is detailed in Figure 4, where boxplots illustrate the distribution of absolute intensities for key lipid species. In line with the observations in individual spectra, DESI consistently yielded higher signal intensities for the majority of lipids. An exception to this pattern was LPC(16:0), where MALDI displayed greater signal intensity.

The assessment of image quality is presented in Figure 5, which presents DESI and MALDI images side-by-side for various lipid classes. To ensure an even comparison of image detail between MALDI and DESI, the images presented are scaled individually to their respective maximum intensities. This approach highlights the potential of each technique for optimal image clarity, while acknowledging that absolute intensity values, as previously demonstrated in mass spectra and boxplot analyses, are inherently higher for DESI than for MALDI. The images acquired via DESI generally provided better contrast and more detailed lipid distributions within the tissue sections. This was contrasted with the MALDI images, which, while informative, appeared less detailed under the same analytical conditions (Figure 5C). In order to substantiate the observation of sharper images obtained with DESI, we computed the two-dimensional autocorrelation function for both DESI and MALDI images. For all masses we investigated, the DESI spatial autocorrelation peak was narrower by a factor 1.5–2, indicating improved feature definition with DESI (Figure S2).

4 | DISCUSSION

In this study, we evaluated the performance of the two prominent ionization techniques for MSI, DESI and MALDI, in detecting lipids within atherosclerotic plaque sections. Atherosclerotic plaques are interesting targets for lipid imaging because their lipid distributions are highly heterogeneous and more variable than those seen in, for instance, rodent brains. The relative abundances of different lipid species and lipid classes in plaque also differ markedly from brain tissue.

Despite lower overall ion count rates, MALDI-MSI facilitated the annotation of a greater number of Cer and HexCer/Hex2Cer species in comparison to DESI-MSI. A possible explanation for this distinction

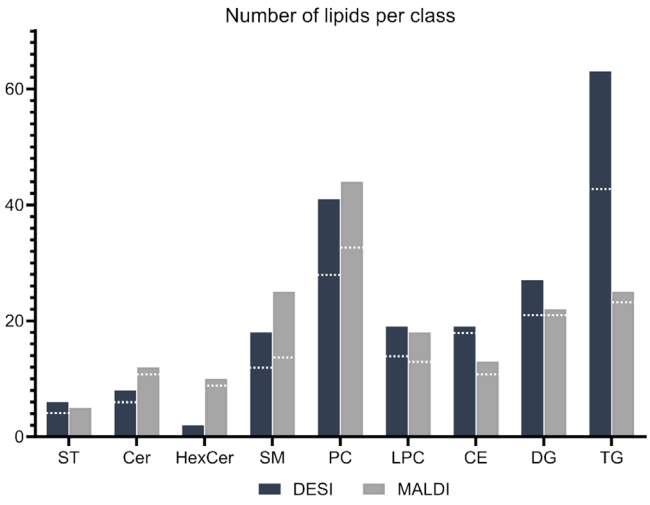

FIGURE 2 Histogram displaying the number of annotated lipids per lipid class for desorption electrospray ionization (DESI) and matrix-assisted laser desorption/ionization (MALDI). The white dashed lines within the bars indicate the total number of unique lipids, signifying annotations counted once regardless of presence in different ion forms. HexCer bars encompass Hex2Cer species. [Color figure can be viewed at wileyonlinelibrary.com]

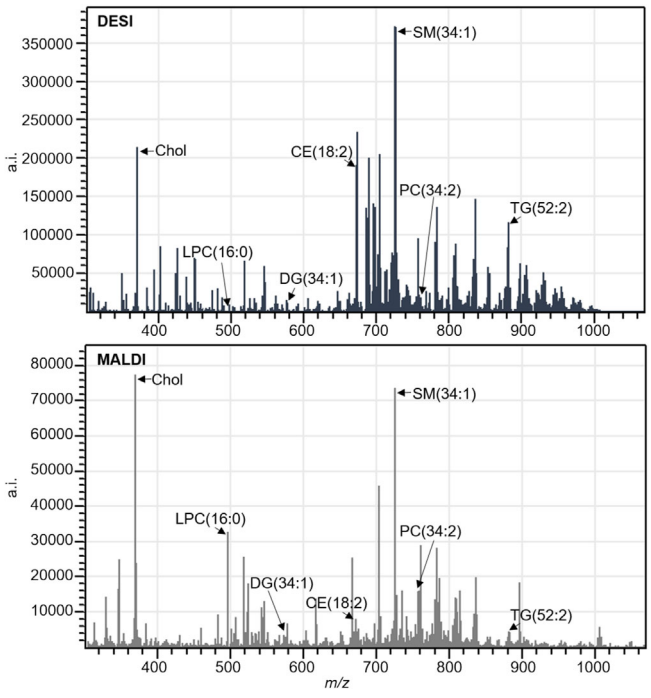

FIGURE 3 Example mass spectra of the same CEA measured by desorption electrospray ionization (DESI) (top) and matrix-assisted laser desorption/ionization (MALDI) (bottom) mass spectrometry imaging (MSI). Several representative lipid species are indicated with arrows. (a.i., absolute intensity; m/z, mass-to-charge ratio) [Color figure can be viewed at wileyonlinelibrary.com]

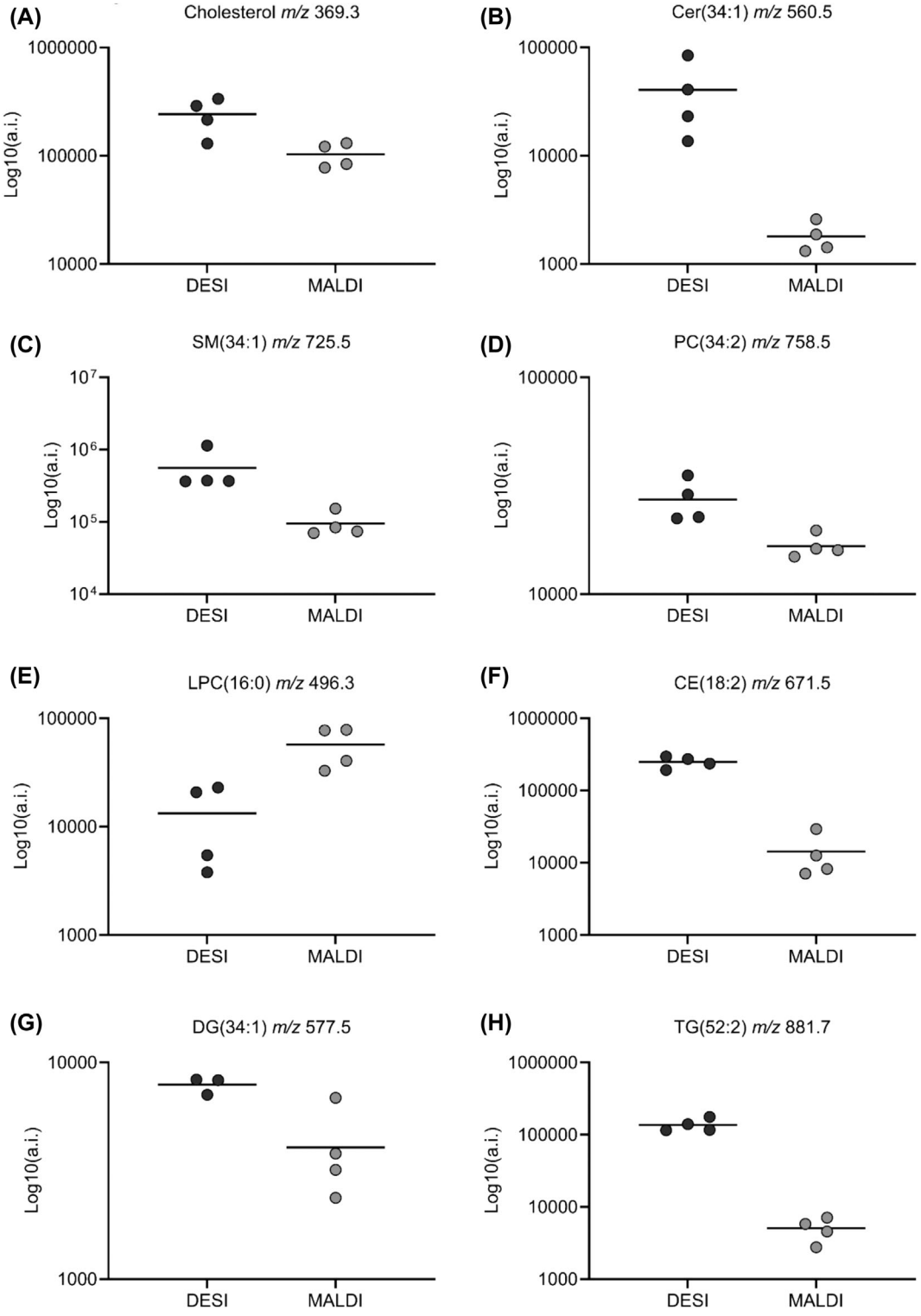

FIGURE 4 Dot plots illustrating the absolute intensities of specific lipids across all four samples, as measured by desorption electrospray ionization (DESI) versus matrix-assisted laser desorption/ionization (MALDI)-mass spectrometry imaging (MSI). Each dot represents an individual sample's absolute intensity (a.i.), and the horizontal line indicates the mean intensity for each group.

lies in the ionization preference, while DESI predominantly detects Cer as [M + Na] + ions, MALDI excels in generating [M + H-H2O] + ions for Cer species.[6] This preference might originate from the energy absorbed and transferred by the laser desorption/ionization process in MALDI, which likely promotes the formation of these dehydrated ions. Consequently, the dehydrated form of Cer is more readily ionized and stabilized in MALDI, enhancing their detection rates and providing a distinct advantage over DESI in identifying these

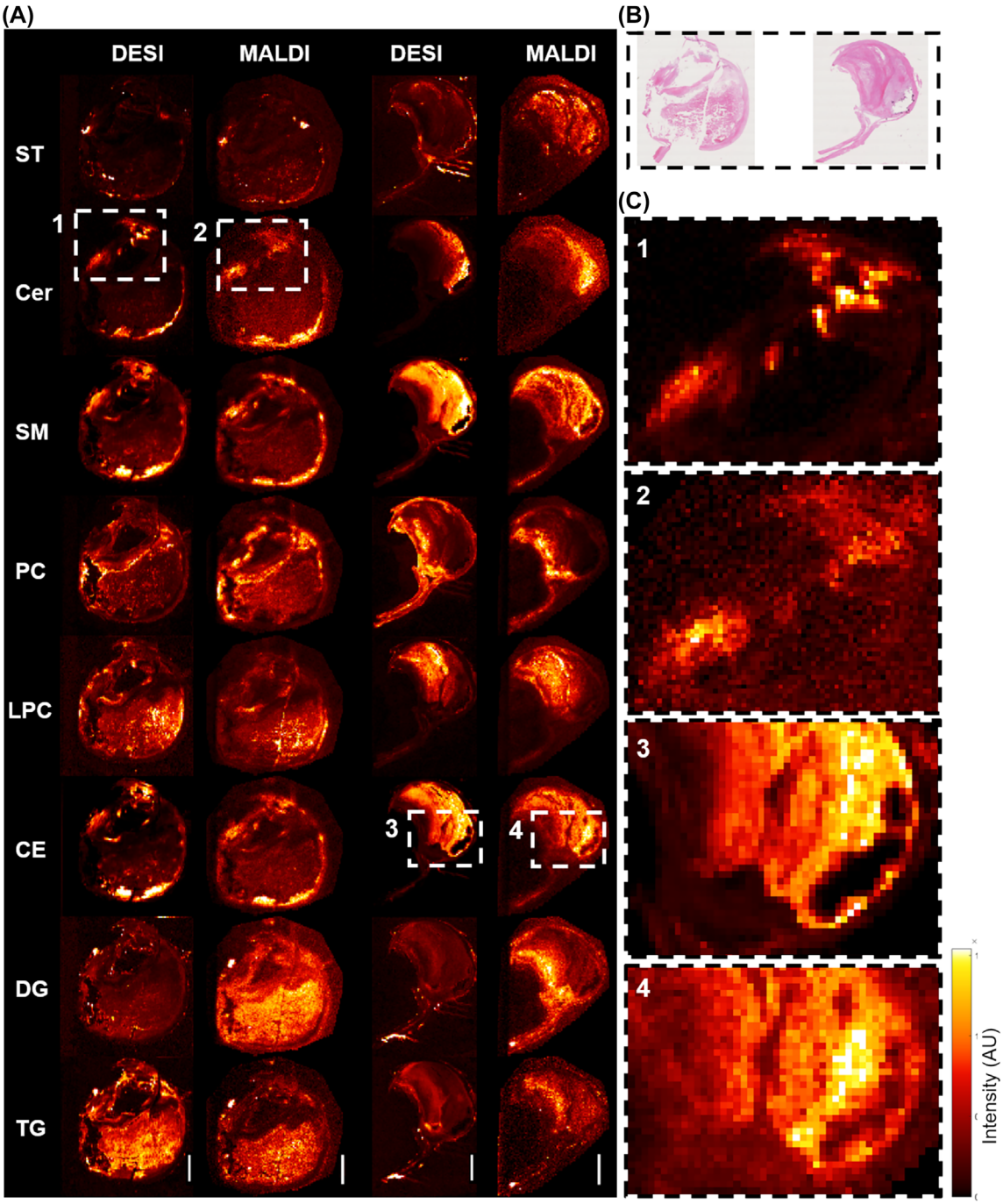

FIGURE 5 Comparative lipid images of carotid plaque sections measured by desorption electrospray ionization (DESI) and matrix-assisted laser desorption/ionization (MALDI)-mass spectrometry imaging (MSI). (A) Side-by-side comparisons of carotid plaque sections analyzed by DESI (left column of each pair) and MALDI (right column of each pair) MSI techniques. A representative m/z feature for each lipid class is depicted, including ST, Cer, SM, PC, LPC, CE, DG, and TG. (B) H&E staining of depicted plaque sections. (C) Zoomed images of regions 1–4 in Figure 4A. Images are scaled to their maximum intensity for optimal image clarity. Scale bars = 1 mm. [Color figure can be viewed at wileyonlinelibrary.com]

species. In addition to the differences in Cer detection, MALDI-MSI also revealed a greater detection of HexCer and Hex2Cer species compared to DESI-MSI. One hypothesis for the reduced detection of these species in DESI could be ion suppression, particularly since HexCer and Hex2Cer ions fall within the same mass range as SM and CE species (for HexCer) and TAG species (for Hex2Cer), which exhibit very high ion count rates in DESI. This high abundance could potentially suppress the ionization of HexCer and Hex2Cer species, leading to their underrepresentation in the detected lipid profile.

Conversely, DESI-MSI was more effective in detecting CE and TG species than MALDI-MSI. A possible cause for the enhanced detection of TG and CE species using DESI-MSI over MALDI-MSI could be

attributed to the differential susceptibility of these lipid classes to fragmentation within the MALDI source.[31] The MALDI process utilizes laser energy for the ionization of analytes, which can induce in-source fragmentation of molecules. Especially larger lipid molecules, such as TGs and CEs, may naturally fragment more readily under the conditions used in MALDI. This fragmentation could potentially compromise the integrity and detectability of TG and CE species in MALDI-MSI. In contrast, the low-energy ionization process of DESI-MSI, which involves directing a charged solvent spray at the sample in an ambient environment, may lead to better preservation of complex lipids, such as TG and CE species.[8,13] Furthermore, the higher signal intensities observed in DESI can be attributed to the larger desorption area and the continuous analyte extraction process from the spray. In contrast, MALDI has a desorption area approximately half the size and analyte extraction occurs during the application of the organic matrix.

Our findings indicate that both ionization techniques are effective in detecting lipids across all major classes present in atherosclerotic plaque. Interestingly, despite previous concerns regarding its sensitivity,[32] DESI-MSI exhibited significantly enhanced overall sensitivity relative to MALDI-MSI. This increased sensitivity in DESI-MSI can be attributed to greater ion suppression in MALDI due to matrix ions, as well as recent technological advancements in the DESI source. These include the adoption of a new focused high-performance sprayer and the implementation of a heated transfer line.[14] These advancements have notably improved the efficiency of ion transfer into the mass spectrometer, thereby elevating the sensitivity of DESI-MSI.[14,15] This enhanced sensitivity has also enabled imaging studies at a markedly higher resolution of 20 × 20 µm pixel size with adequate count rate by DESI imaging of lipids in atherosclerotic plaque.[24]

For most images, DESI-MSI produced more detailed lipid distributions than MALDI-MSI. This improvement can be attributed to DESI's direct tissue surface sampling, which eliminates the need for matrix application. The application of a matrix by spraying in MALDI-MSI has the potential to cause analytes to delocalize. This matrix-induced delocalization can result in less defined images, as the molecules "float" and spread out from their original locations.[33] However, matrix sublimation offers a potential remedy for this issue, presenting a method that minimizes the risk of lipid delocalization by providing a more controlled application of the matrix.[34]

The primary focus of this study was to assess the comparative performance of DESI and MALDI ionization techniques for lipid detection in atherosclerotic plaques. However, it is important to recognize the established biological significance of lipid mapping in atherosclerosis. Lipids play pivotal roles in the development and progression of atherosclerosis,[35–38] and their precise localization can provide insights into the mechanisms driving plaque formation, progression, and potential instability. Previous research has shown that using MSI to study lipids within atherosclerotic plaque has profound implications for understanding the pathophysiology of the disease.[17–24]

In conclusion, our study found that both MALDI and DESI are highly suitable techniques for detecting a wide range of lipids in atherosclerotic plaque sections. Furthermore, we observed that DESI-MSI exhibited higher sensitivity for most lipid classes than MALDI-MSI and provided images with improved feature definition compared to MALDI in these tissues. For some lipid classes of interest, such as Cer and HexCer, MALDI-MSI allowed annotation of a greater number of species. These results highlight the suitability of DESI for lipidomic imaging in heterogeneous samples and confirm its complementarity to MALDI as a valuable method for MSI.

AUTHOR CONTRIBUTIONS

Nuria Slijkhuis: Writing—original draft; project administration; investigation; software; formal analysis; visualization; conceptualization; data curation; methodology; validation. **Mark Towers:** Conceptualization; methodology; writing—review and editing; resources; software; data curation; investigation; visualization. **Emmanuelle Claude:** Conceptualization; writing—review and editing; resources; methodology. **Gijs van Soest:** Funding acquisition; writing—review and editing; conceptualization; resources; supervision; validation; project administration.

PEER REVIEW

The peer review history for this article is available at https://www.webofscience.com/api/gateway/wos/peer-review/10.1002/rcm.9927.

DATA AVAILABILITY STATEMENT

The data that support the findings of this study are available from the corresponding author upon reasonable request.

ORCID

Nuria Slijkhuis https://orcid.org/0000-0002-6922-2045

REFERENCES

1. Lv J, Zhang L, Yan F, Wang X. Clinical lipidomics: A new way to diagnose human diseases. *Clin Transl Med*. 2018;7(1):12. doi:10.1186/s40169-018-0190-9
2. Zhao YY, Cheng XL, Lin RC. Lipidomics applications for discovering biomarkers of diseases in clinical chemistry. *Int Rev Cell Mol Biol*. 2014;313:1-26. doi:10.1016/B978-0-12-800177-6.00001-3
3. Chughtai K, Heeren RM. Mass spectrometric imaging for biomedical tissue analysis. *Chem Rev*. 2010;110(5):3237-3277. doi:10.1021/cr100012c
4. Cornett DS, Reyzer ML, Chaurand P, Caprioli RM. MALDI imaging mass spectrometry: Molecular snapshots of biochemical systems. *Nat Methods*. 2007;4(10):828-833. doi:10.1038/nmeth1094
5. Norris JL, Caprioli RM. Analysis of tissue specimens by matrix-assisted laser desorption/ionization imaging mass spectrometry in biological and clinical research. *Chem Rev*. 2013;113(4):2309-2342. doi:10.1021/cr3004295
6. Zemski Berry K, Hankin J, Barkley R, Spraggins J, Caprioli RM, Murphy RC. MALDI imaging of lipid biochemistry in tissues by mass spectrometry. *Chem Rev*. 2011;111(10):6491-6512. doi:10.1021/cr200280p
7. Keller C, Maeda J, Jayaraman D, et al. Comparison of vacuum MALDI and AP-MALDI platforms for the mass spectrometry imaging of metabolites involved in salt stress in *Medicago truncatula*. *Front Plant Sci*. 2018;9:1238. doi:10.3389/fpls.2018.01238
8. Skraskova K, Claude E, Jones EA, Towers M, Ellis SR, Heeren RM. Enhanced capabilities for imaging gangliosides in murine brain with matrix-assisted laser desorption/ionization and desorption electrospray

ionization mass spectrometry coupled to ion mobility separation. *Methods*. 2016;104:69-78. doi:10.1016/j.ymeth.2016.02.014
9. Takáts Z, Wiseman JM, Gologan B, Cooks RG. Mass spectrometry sampling under ambient conditions with desorption electrospray ionization. *Science*. 2004;306(5695):471-473. doi:10.1126/science.1104404
10. Eberlin LS, Ferreira CR, Dill AL, Ifa DR, Cooks RG. Desorption electrospray ionization mass spectrometry for lipid characterization and biological tissue imaging. *Biochim Biophys Acta Mol Cell Biol Lipids*. 2011;1811(11):946-960. doi:10.1016/j.bbalip.2011.05.006
11. Takats Z, Wiseman JM, Cooks RG. Ambient mass spectrometry using desorption electrospray ionization (DESI): Instrumentation, mechanisms and applications in forensics, chemistry, and biology. *J Mass Spectrom*. 2005;40(10):1261-1275. doi:10.1002/jms.922
12. Dill AL, Ifa DR, Manicke NE, Ouyang Z, Cooks RG. Mass spectrometric imaging of lipids using desorption electrospray ionization. *J Chromatogr B Analyt Technol Biomed Life Sci*. 2009;877(26):2883-2889. doi:10.1016/j.jchromb.2008.12.058
13. Ifa DR, Wu C, Ouyang Z, Cooks RG. Desorption electrospray ionization and other ambient ionization methods: Current progress and preview. *Analyst*. 2010;135(4):669-681. doi:10.1039/b925257f
14. Claude E, Towers M, Jones E. Update DESI mass spectrometry imaging (MSI). In: Cole LM, Clench MR, eds. *Imaging mass spectrometry methods in molecular biology*. *2688*. Humana; 2023. doi:10.1007/978-1-0716-3319-9_4
15. Morato NM, Cooks RG. Inter-platform assessment of performance of high-throughput desorption electrospray ionization mass spectrometry. *Talanta Open*. 2021;4:100046. doi:10.1016/j.talo.2021.100046
16. Ross R. Atherosclerosis—an inflammatory disease. *N Engl J Med*. 1999;340(2):115-126. doi:10.1056/NEJM199901143400207
17. Moerman AM, Visscher M, Slijkhuis N, et al. Lipid signature of advanced human carotid atherosclerosis assessed by mass spectrometry imaging. *J Lipid Res*. 2021;62:100020. doi:10.1194/jlr.RA120000974
18. Cao J, Goossens P, Martin-Lorenzo M, et al. Atheroma-specific lipids in ldlr(−/−) and apoe(−/−) mice using 2D and 3D matrix-assisted laser desorption/ionization mass spectrometry imaging. *J am Soc Mass Spectrom*. 2020;31(9):1825-1832. doi:10.1021/jasms.0c00070
19. Zaima N, Sasaki T, Tanaka H, et al. Imaging mass spectrometry-based histopathologic examination of atherosclerotic lesions. *Atherosclerosis*. 2011;217(2):427-432. doi:10.1016/j.atherosclerosis.2011.03.044
20. Greco F, Quercioli L, Pucci A, et al. Mass spectrometry imaging as a tool to investigate region specific lipid alterations in symptomatic human carotid atherosclerotic plaques. *Metabolites*. 2021;11(4):250. doi:10.3390/metabo11040250
21. Slijkhuis N, Razzi F, Korteland SA, et al. Spatial Lipidomics of coronary atherosclerotic plaque development in a familial hypercholesterolemia swine model. *J Lipid Res*. 2024;65(2):100504. doi:10.1016/j.jlr.2024.100504
22. Manicke NE, Nefliu M, Chunping W, et al. Imaging of lipids in atheroma by desorption electrospray ionization mass spectrometry. *Anal Chem*. 2009;81(21):8702-8707. doi:10.1021/ac901739s
23. Li W, Luo J, Peng F, et al. Spatial metabolomics identifies lipid profiles of human carotid atherosclerosis. *Atherosclerosis*. 2023;364:20-28. doi:10.1016/j.atherosclerosis.2022.11.019
24. Slijkhuis N, Towers M, Mirzaian M, et al. Identifying lipid traces of atherogenic mechanisms in human carotid plaque. *Atherosclerosis*. 2023;385:117340. doi:10.1016/j.atherosclerosis.2023.117340
25. Barré F, Rocha B, Dewez F, et al. Faster raster matrix-assisted laser desorption/ionization mass spectrometry imaging of lipids at high lateral resolution. *Int J Mass Spectrom*. 2019;437:38-48. doi:10.1016/j.ijms.2018.09.015
26. Towers M, Jones E, Ballantyne J, Jarvis S, eds. High resolution low flow DESI imaging using a commercial DESI source. 72nd ASMS conference on mass spectrometry and allied topics. 2024; Anaheim, California.
27. Jones EA, Hoyes E, Trinkle S, Chapman R, eds. DESI imaging at the cellular level through the application of nano-flow and multi-focus approaches 71st ASMS conference on mass spectrometry and allied topics. 2023.
28. Visscher M, Moerman AM, Burgers PC, et al. Data processing pipeline for lipid profiling of carotid atherosclerotic plaque with mass spectrometry imaging. *J Am Soc Mass Spectrom*. 2019;30(9):1790-1800. doi:10.1007/s13361-019-02254-y
29. Strohalm M, Hassman M, Košata B, Kodíček M. mMass data miner: An open source alternative for mass spectrometric data analysis. *Rapid Commun Mass Spectrom*. 2008;22(6):905-908. doi:10.1002/rcm.3444
30. Ghorasaini M, Mohammed Y, Adamski J, et al. Cross-laboratory standardization of preclinical lipidomics using differential mobility spectrometry and multiple reaction monitoring. *Anal Chem*. 2021;93(49):16369-16378. doi:10.1021/acs.analchem.1c02826
31. Al-Saad KA, Zabrouskov V, Siems WF, Knowles NR, Hannan RM, Hill HH Jr. Matrix-assisted laser desorption/ionization time-of-flight mass spectrometry of lipids: Ionization and prompt fragmentation patterns. *Rapid Commun Mass Spectrom*. 2003;17(1):87-96. doi:10.1002/rcm.858
32. He MJ, Pu W, Wang X, Zhang W, Tang D, Dai Y. Comparing DESI-MSI and MALDI-MSI mediated spatial metabolomics and their applications in cancer studies. *Front Oncol*. 2022;12:891018. doi:10.3389/fonc.2022.891018
33. Gemperline E, Rawson S, Li L. Optimization and comparison of multiple MALDI matrix application methods for small molecule mass spectrometric imaging. *Anal Chem*. 2014;86(20):10030-10035. doi:10.1021/ac5028534
34. Thomas A, Charbonneau JL, Fournaise E, Chaurand P. Sublimation of new matrix candidates for high spatial resolution imaging mass spectrometry of lipids: Enhanced information in both positive and negative polarities after 1,5-diaminonapthalene deposition. *Anal Chem*. 2012;84(4):2048-2054. doi:10.1021/ac2033547
35. Cheng JM, Suoniemi M, Kardys I, et al. Plasma concentrations of molecular lipid species in relation to coronary plaque characteristics and cardiovascular outcome: Results of the ATHEROREMO-IVUS study. *Atherosclerosis*. 2015;243(2):560-566. doi:10.1016/j.atherosclerosis.2015.10.022
36. Edsfeldt A, Dunér P, Stahlman M, et al. Sphingolipids contribute to human atherosclerotic plaque inflammation. *Arterioscler Thromb Vasc Biol*. 2016;36(6):1132-1140. doi:10.1161/ATVBAHA.116.305675
37. Jové M, Ayala V, Ramírez-Núñez O, et al. Lipidomic and metabolomic analyses reveal potential plasma biomarkers of early atheromatous plaque formation in hamsters. *Cardiovasc Res*. 2013;97(4):642-652. doi:10.1093/cvr/cvs368
38. Zelnik ID, Kim JL, Futerman AH. The complex tail of circulating sphingolipids in atherosclerosis and cardiovascular disease. *J Lipid Atheroscler*. 2021;10(3):268-281. doi:10.12997/jla.2021.10.3.268

SUPPORTING INFORMATION

Additional supporting information can be found online in the Supporting Information section at the end of this article.

How to cite this article: Slijkhuis N, Towers M, Claude E, van Soest G. MALDI versus DESI mass spectrometry imaging of lipids in atherosclerotic plaque. *Rapid Commun Mass Spectrom*. 2025;39(1):e9927. doi:10.1002/rcm.9927